Carnegie Mellon University
Research Showcase @ CMU

Department of Mechanical Engineering | Carnegie Institute of Technology

1991

New design paradigms for SISO control system synthesis

Thomas R. Kurfess
Carnegie Mellon University

Mark L. Nagurka

Carnegie Mellon University.Engineering Design Research Center.

Follow this and additional works at: http://repository.cmu.edu/meche

This Technical Report is brought to you for free and open access by the Carnegie Institute of Technology at Research Showcase @ CMU. It has been accepted for inclusion in Department of Mechanical Engineering by an authorized administrator of Research Showcase @ CMU. For more information, please contact research-showcase@andrew.cmu.edu.

NOTICE WARNING CONCERNING COPYRIGHT RESTRICTIONS:
The copyright law of the United States (title 17, U.S. Code) governs the making of photocopies or other reproductions of copyrighted material. Any copying of this document without permission of its author may be prohibited by law.

New Design Paradigms for SISO Control System Synthesis

by

Thomas R. Kurfess, Mark L. Nagurka

EDRC 24-49-91

New Design Paradigms for SISO Control System Synthesis

T.R. Kurfess and MX. **Nagurka**
Department of Mechanical Engineering
Carnegie Mellon University
Pittsburgh, PA 15213

March 1991

This paper proposes a new graphical representation and perspective on the Evans root locus, a well known controls technique for stability and performance evaluation. The visualization is based on the adjustment of a proportional control gain in the same fashion that is employed in constructing the root locus. The result is a set of Gain Plots (GPs) depicting the root loci in polar coordinates, i.e., magnitude and angle, of each closed loop system eigenvalue in the complex plane as a function of the gain.

The GPs impart significant insight for determining the values of gain that render a closed-loop system either stable or unstable. By exposing the correspondence of gain values to specific eigenvalues, the GPs are a useful pole-placement tool for identifying closed-loop designs meeting performance specifications. An additional advantage of the GPs is their ability to reveal by inspection information about the gain sensitivity of closed-loop eigenvalues.

This paper develops the concept of GPs and applies them to single-input, single-output (SISO) systems. A companion paper (Nagurka and Kurfess, 1991a) extends the concepts to multivariable closed-loop feedback systems. For both cases, the GPs present eigenvalue trajectories in an informative and unambiguous manner.

University Libraries
Carnegie Motion University
Pittsburgh PA 15213-3890

Introduction

In a sequence of two landmark papers, W.R. Evans presented a technique for analyzing and graphically portraying the loci of closed-loop system poles (Evans, 1948, 1950). Since the publication of these papers, the Evans root locus technique has become a standard and commonly employed tool of the control engineer. The root locus plot has several qualities that make it a valuable classical controls tool; perhaps its most valued assets are the ease with which it may be implemented and the tremendous amount of information and insight that it provides.

For most single-input, single-output (SISO) linear time-invariant systems, sketching the root locus as a function of gain is a simple and well documented task. Most undergraduate controls textbooks present the sketching rules for constructing the root locus plot By following these rules, the loci of roots - or system eigenvalues - may be graphed in the complex plane as certain parameters are varied Although the rules are applicable to any real valued parameters, the most common parameter investigated is the proportional control gain. In accordance with convention, this is the parameter studied in this report. Although it may not be exact, the approximate root locus plot provides a plethora of useful information about system stability and performance. For example, closed-loop stability can be determined, and damping and response speed can be estimated as the gain is varied.

This report promotes an alternate graphical representation of the root locus plot that exposes the relationship between the pole locations and the gain without sacrificing any of the information presented in the standard root locus. The representation, based on the same variable gain analysis employed by Evans, is summarized by a pair of Gain Plots (GPs) that casts the magnitude and angle of the system eigenvalues in the complex plane as an explicit function of gain. By utilizing an eigenvalue polar representation, the GPs present system performance information such as damping and natural frequency in a clear and concise manner, and, as such, serve as a new graphical pole-placement tool. Additionally, gain sensitivity of the closed-loop eigenvalues can be obtained by examining the slopes of the magnitude and angle plots with changing gain. The GPs can be constructed for, and are applicable to, both SISO and multiple-input, multiple-output (MIMO) systems.

This report specifically addresses SISO systems as covered in "classical controls/' Multivariable systems are considered in a companion report (Nagurka and Kurfess, 1991a). For purposes of illustration, the open-loop transfer function, g(s),

$$g(s) = \frac{(s+3)}{(s+1)(s+2)} \tag{1}$$

is used as a **"theme" example** in the following two sections. This transfer function is embedded in a standard closed-loop negative feedback system shown in Figure (1).

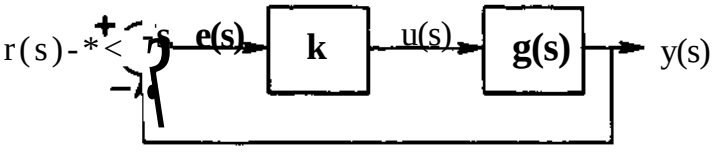

Figure 1. Closed-Loop SISO Negative Feedback Configuration.

The report is organized as follows. A conceptual framework that motivates the development of the GPs is presented in the next two sections. First, the development of *classical frequency-domain* techniques is unfolded via a sequence of novel and intriguing three-dimensional representations; then, in parallel fashion, a sequence of *gain-domain* methods is proposed. A subsequent section describes important properties and advantages of GPs that make them such a rich design tool. A non-trivial SISO example, that demonstrates the utility of the GPs for stability, performance, and gain sensitivity analyses, is then solved. Finally, a high-level perspective, suggesting a framework that locks together three key classical control tools and the GPs, is discussed in the closing section of this report The highlights of this unifying framework are summarized in Figure 2.

Frequency-Domain Conceptualization

This section presents a unified framework for viewing classical control frequency-domain tools such as the Nyquist diagram and Bode plots. The premise is that the Bode plots present the information of the Nyquist diagram in an enhanced perspective by exposing frequency explicitly. Furthermore, the Bode plots are the result of a natural progression of perspectives on the classical Nyquist diagram. Although this progression does not necessarily reflect the chronological unfolding of events, it serves as a useful paradigm that logically bridges the fundamental frequency-domain tools of classical controls. This transition from the Nyquist diagram to two different three-dimensional representations, including one that reveals the classical Bode plots via orthogonal views, is summarized in Figure 3.

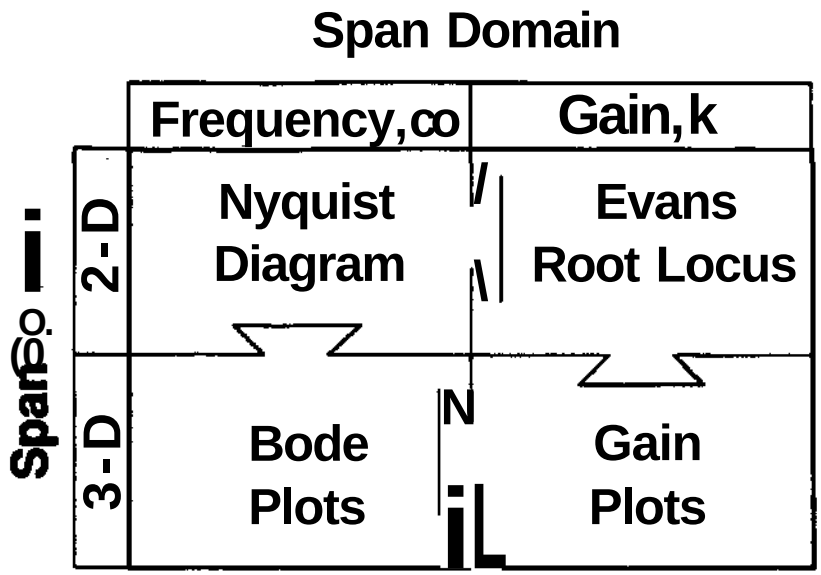

Figure 2. Assembling the Controls Tool Puzzle.

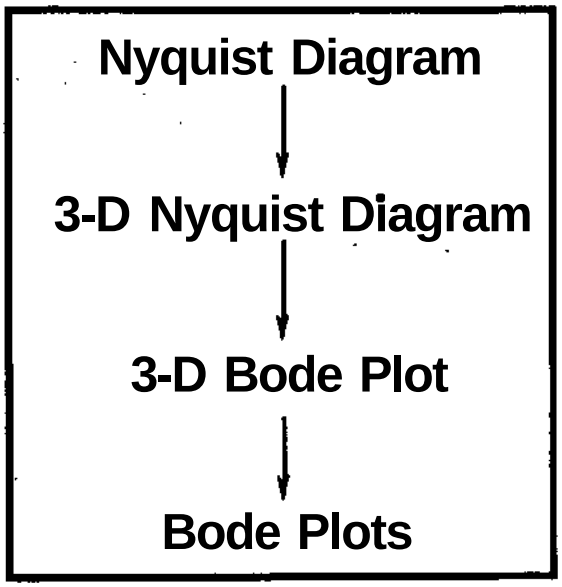

Figure 3. Progression of Frequency-Domain Tools.

Later in this report, it is shown that this development of the Bode plots from the Nyquist diagram is paralleled by the development of the GPs from the Evans root locus plot As such, fundamental relationships appear to exist between the Nyquist diagram, the Bode plots, the Evans root locus, and the GPs.

The Nyquist Diagram (Nyquist, 1932)

The Nyquist diagram is a polar plot of a sinusoidal transfer function, g(jco), graphed over the range

$$0 \pounds C0 < \infty \qquad \pounds)$$

(The lower limit of equation (2) can alternatively be chosen as -o©, with the resulting curve being symmetric about the real axis.) Although the Nyquist diagram is a polar representation, it is graphed in a complex Cartesian plane where the implicit variable is co. Figure 4 is the Nyquist diagram of equation (1) for co given by equation (2). The Nyquist curve starts at co=O corresponding to a D.C. gain magnitude of 1.5 and phase angle of $0^{\#}$, and asymptotically approaches the origin (zero magnitude) from -90*.

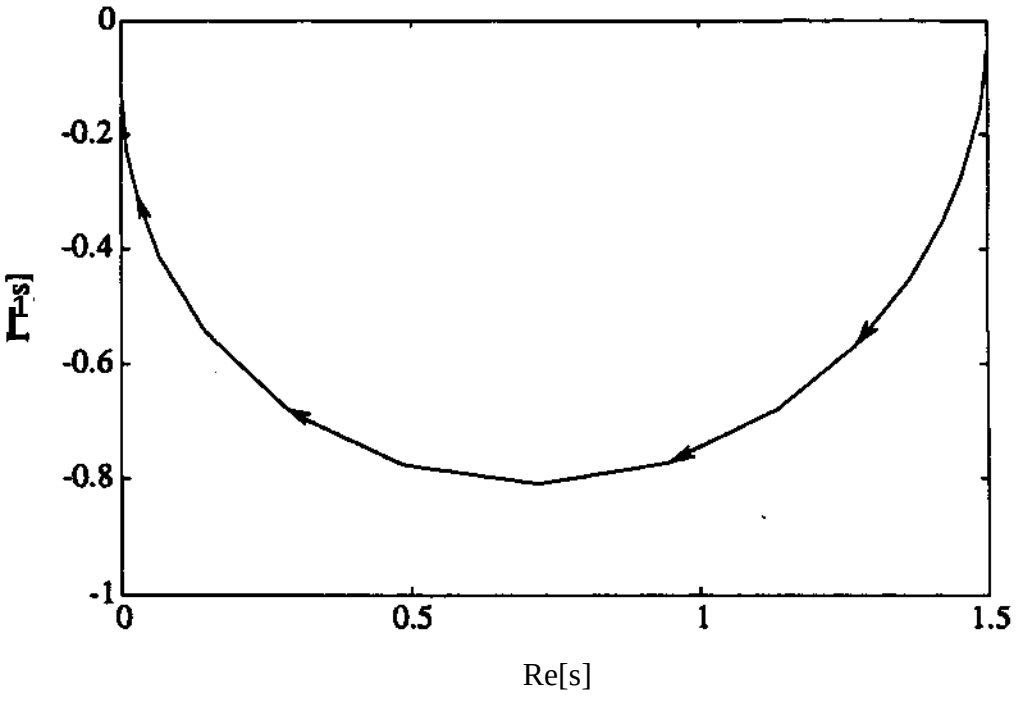

Figure 4. The Nyquist Diagram of Equation (1).

It is possible to show the frequency graduation on the locus (with tick marks denoting equal values of co) or to present superimposed constant frequency contours (Ogata, 1990). However, even if these are added, it is not convenient to identify the frequency associated with a given point on the Nyquist diagram.

Three-Dimensional Nyquist Diagram

The Nyquist diagram can be conceptualized as a two-dimensional "collapsed" perspective of a three-dimensional curve, as shown in Figure 5 for the transfer function of equation (1). In this representation, two of the axes remain the same as in the Nyquist diagram, *i.e.*, real and imaginary components, and a third axis is added to denote the frequency, co. Note that as CD->°O the curve approaches the origin of the complex plane. Although the three-dimensional curve is one means to incorporate frequency information into the Nyquist diagram, it does not present the controls engineer with an intuitive feel for the system behavior, partly because of the difficulty in following the contour and in extracting coordinate information.

Three-Dimensional Bode Plot

An alternative three-dimensional representation can be conceptualized that maps the real and complex components of g(s) to magnitude and angle components. Here, the complex transfer function, g(s), is written as

$$g(s) = Re[g(s)] + jIm[g(s)] = |g(s)|e^{j\angle g(s)} \tag{3}$$

where the transfer function angle and magnitude are given, respectively, as

$$Zg(s>= \tan\text{-}H/m[g(s)],*e[g(s)]) \tag{4}$$

$$|g(s)| = \sqrt{\{Re[g(s)]\}2 + \{/m[g(s)]\}^2} \tag{5}$$

where Zg(s) in equation (4) is given by the two argument inverse tangent function.

Equations (4) and (5) can be used to transform Figure 5 into Figure 6, showing the effect of frequency on the magnitude and angle of the open-loop system given by equation (1). Clearly, this three-dimensional curve is related to well-known variable frequency plots mentioned in the literature (Bode, 1940).

The Bode Plots (Bode, 1940)

The Bode plots consist of two planar plots, one called the Bode magnitude plot showing magnitude *vs.* frequency, and the second called the Bode angle (or phase) plot reporting angle *vs.* frequency. Figures 7a,b are the Bode magnitude and angle plots for the open-loop system given by equation (1).

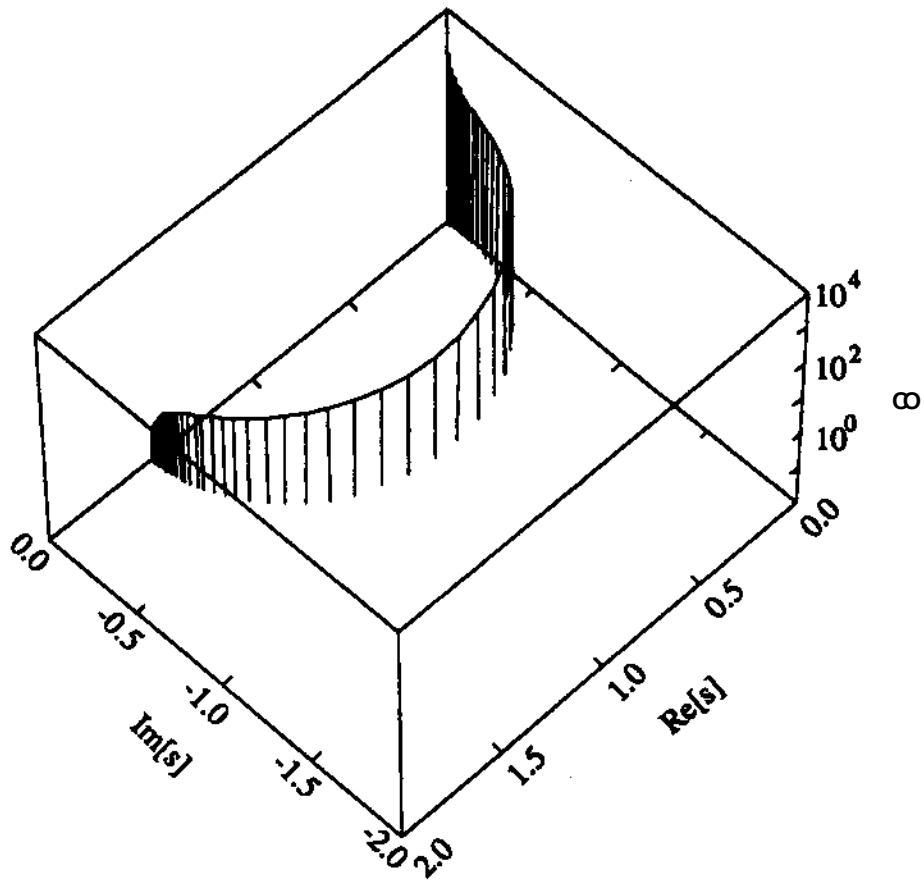

Figure 5. Three-Dimensional Nyquist Diagram of Equation (1).

The Bode plots represent two orthogonal views of the three-dimensional Bode plot of Figure 6, *i.e.*, the Bode magnitude plot is seen by observing Figure 6 from a direction orthogonal to the o-magnitude plane and the Bode angle plot is seen by viewing Figure 6 from a direction orthogonal to the co-angle plane. (In fact, Figures 6 and 7 were generated using the identical data set) Although the same information is presented in Figures 6 and 7, the traditional Bode plots are significantly simpler to understand. Indeed, Bode plots are among the control engineers[9] most powerful tools.

Gain-Domain Conceptualization

In analogous fashion to the frequency-domain progression, the development of the GP's follows a gain-domain evolution beginning with the Evans root locus plot. The traditional two-dimensional root locus plot is then complemented by a third axis representing the gain. The resulting three-dimensional plot is conformally mapped into a new space that presents polar coordinate information associated with the complex plane.

The GPs are the result of two orthogonal views of this new three-dimensional space A summary of this development is traced in Figure 8.

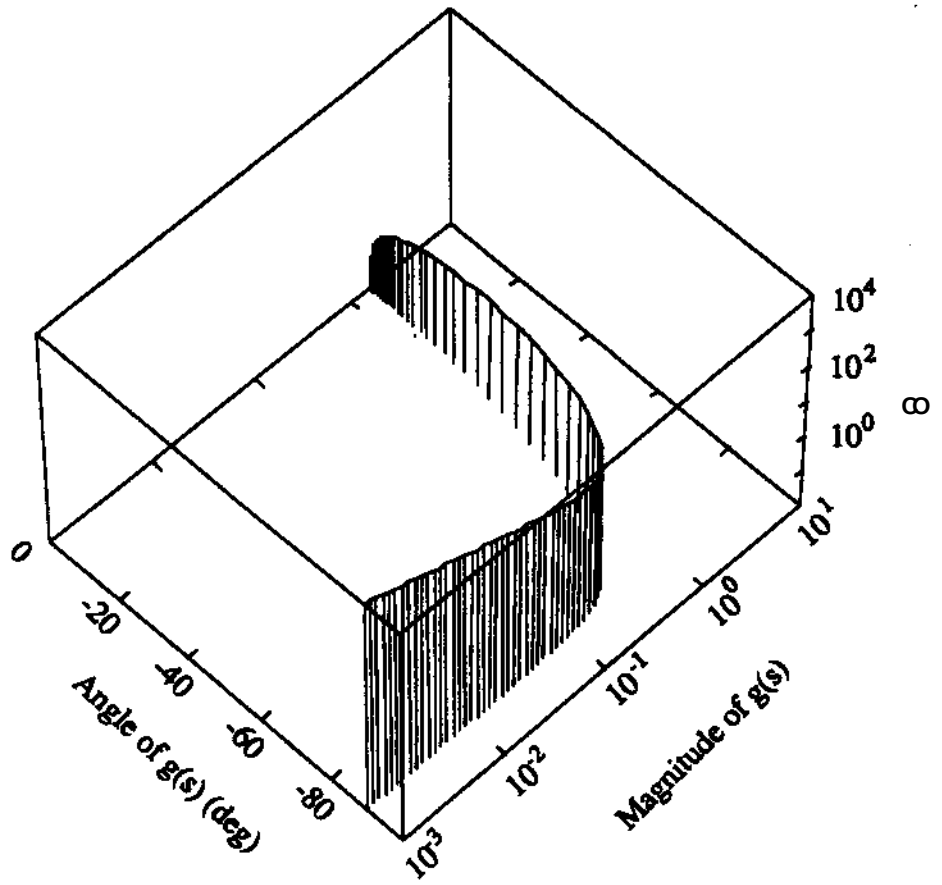

Figure 6. Three-Dimensional Bode Plot of Equation (1).

The Evans Root Locus (Evans, 1948, 1950)

The root locus plot drawn in the complex plane shows the location of the characteristic roots, i.e., the eigenvalues, in terms of some (real valued) system parameter such as the proportional gain. It is based on the closed-loop transfer function of Figure 3 given by

$$\frac{g(s)}{1+kg(s)} \qquad \textbf{(6)}$$

where k is the proportional gain. The stability of the closed-loop system is determined by the eigenvalues, *i.e.*, the denominator roots of equation (6).

$$kg(s) = -1 \qquad (7)$$

The ropt locus is the solution set of equation (7) as the gain k varies in the range

$$0 \le k < \infty \tag{8}$$

Equation (8) is equivalent to two conditions: the angle criterion,

$$Zkg(s) = \pm 180^{\#}(2m + 1), \quad m = 0,1,2, \ldots \tag{9}$$

and the magnitude criterion,

$$|kg(s)| = 1 \tag{10}$$

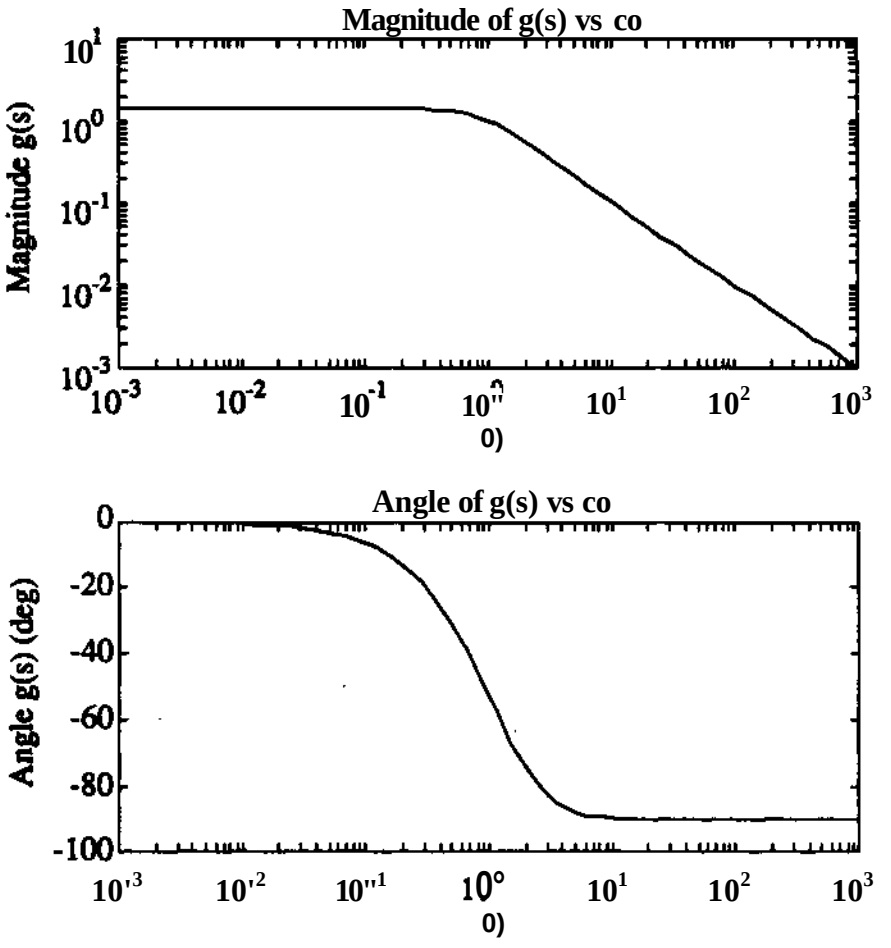

Figure 7a,b. The Bode Plots of Equation (1).

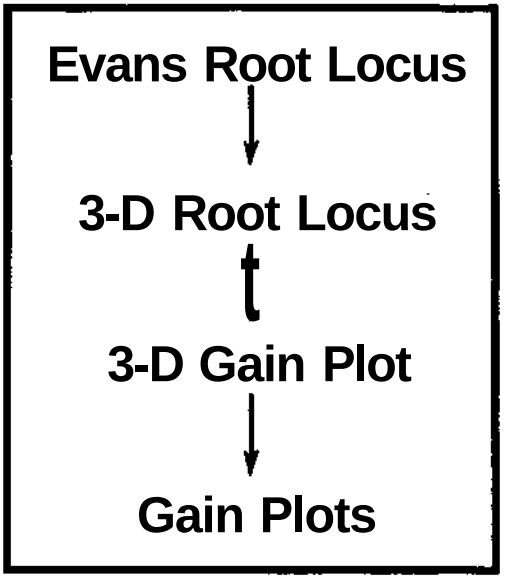

Figure 8. Progression of Gain-Domain Tools.

The shape of the root locus plot is determined entirely by the angle criterion. Then, for any eigenvalue s on the root locus, the magnitude criterion is invoked to solve for the corresponding value of k. (This process is referred to as scaling the locus.) Figure 9 is the root locus plot of equation (1) for k given by equation (8). Each branch of the root locus starts at k=0 corresponding to a system open-loop pole, and asymptotically approaches either a finite or infinite transmission zero. It is possible to show the gain graduation on the locus (with tick marks denoting equal values of k) or to present superimposed constant gain contours.

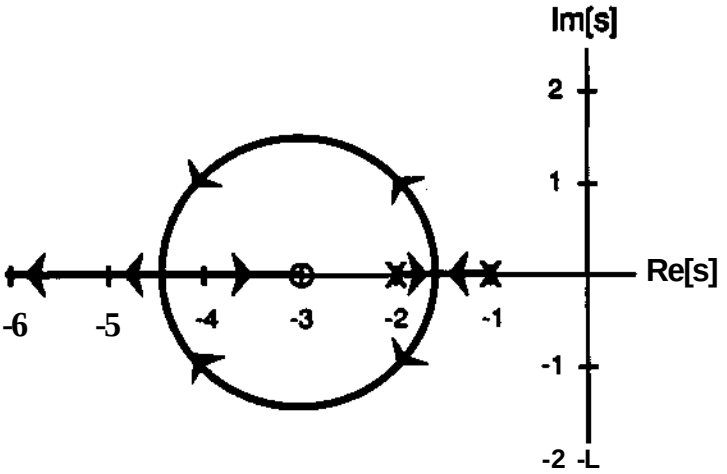

Figure 9. Evans Root Locus Plot of Equation (1).

The root locus gives a direct indication of closed-loop system instability by observing **branches** that enter the right half complex plane (indicating positive real-part eigenvalues). Hence* by inspection, it is possible to determine the stability of the closed-loop system as as **the** gain varies. In addition, the root locus plot is a graphical performance tool providing metrics of natural frequency (On) and damping ratio (£). These two characteristics, known from magnitude and angle information in the Cartesian plane, enable the calculation of many critical performance indices (damped natural frequency, system time constants, *etc.)* It follows that the root locus plot may be viewed as a polar representation graphed in a complex Cartesian plane where the implicit variable is k. In summary, insight into the performance characteristics requires "polar coordinate" information from the root locus.

As noted above, the shape of the root locus plot is based completely on the angle criterion. This presents difficulties for using the root locus plot for direct evaluation of gain. It was also noted that it is possible to reconstruct - via scaling - the implicit parameter k from the root locus magnitude criterion. However, even if this is done (and tick marks denoting values of k are added to the locus), it is not convenient to determine the gain associated with a specific point on the locus using the traditional root locus plot. For example, from Figure 9 the gain k « 5.8 generating the break-in point at s * -4.4 cannot (readily) be determined by inspection. It will be shown that an alternate graphical representation may be employed to circumvent this difficulty.

Three-Dimensional Root Locus

Just as the Nyquist diagram can be extended by adding a frequency axis, the Evans root locus plot can be presented in three-dimensional space where the real and imaginary axes of the s-plane comprise two of the dimensions, and the gain, k, is added as a third axis. Figure 10 presents such a three-dimensional root locus for the closed-loop system of Figure 3 with open-loop transfer function of equation (1). The original Evans root locus is the projection of this three-dimensional locus onto the real-imaginary plane. The idea for adding a third dimension for gain was suggested by Cannon (1967) in depicting a break-point as a saddle point. Two saddle points may be seen in Figure 10. Again, the portrayal of three-dimensional information does not provide the controls engineer with an intuitive feel for system behavior.

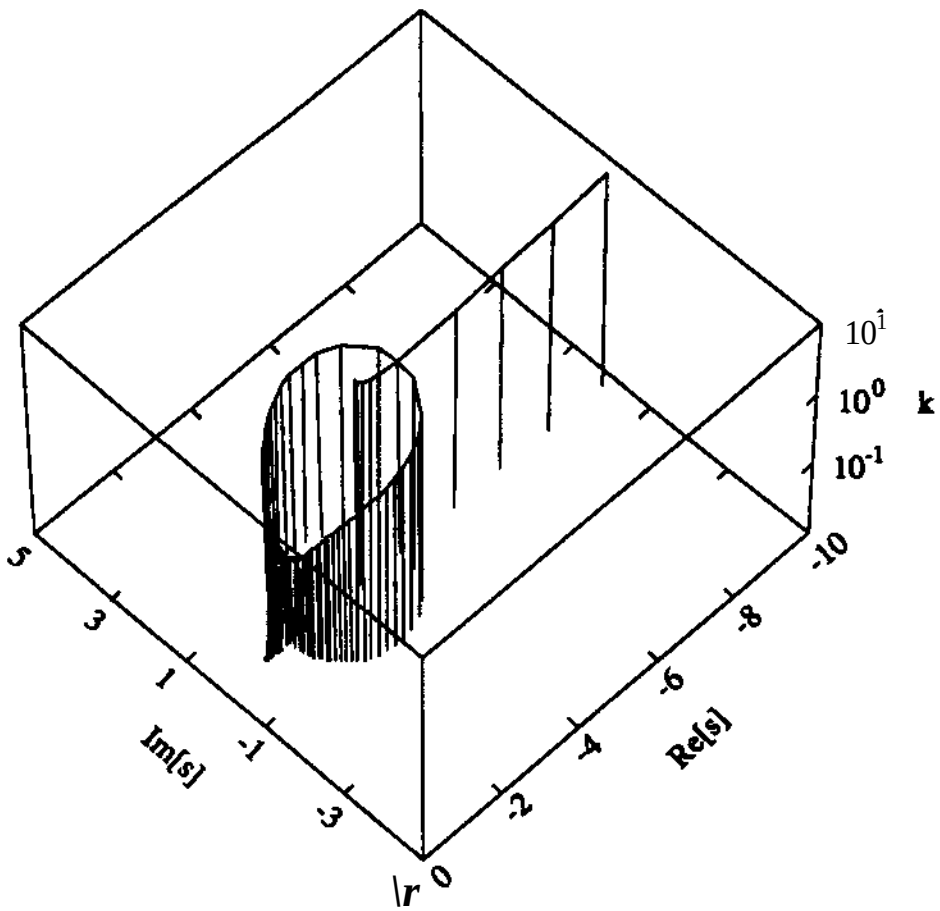

Figure 10. Three-dimensional Root Locus Diagram of Equation (1).

Three-Dimensional Gain Plots

The three-dimensional representation described above can be viewed alternatively by mapping the real and complex components to magnitude and angle components. Here, the complex value, s, is expressed as

$$s = \sigma + j\omega = Re^{j\theta} \tag{11}$$

where the angle, 6, and magnitude, R, are

$$6 = \tan^{-1}(\omega, \sigma) \tag{12}$$

$$R = \sqrt{\sigma^2 + \omega^2} \tag{13}$$

In equation (12) 9 is given by the two argument inverse tangent function.

Equations (12) and (13) can be used to transform Figure 10 into Figure 11 showing the effect **of gain** on the magnitude and angle of the closed-loop system given by equation (3). This three-dimensional curve, still related to the root-locus diagram, is difficult to visualize.

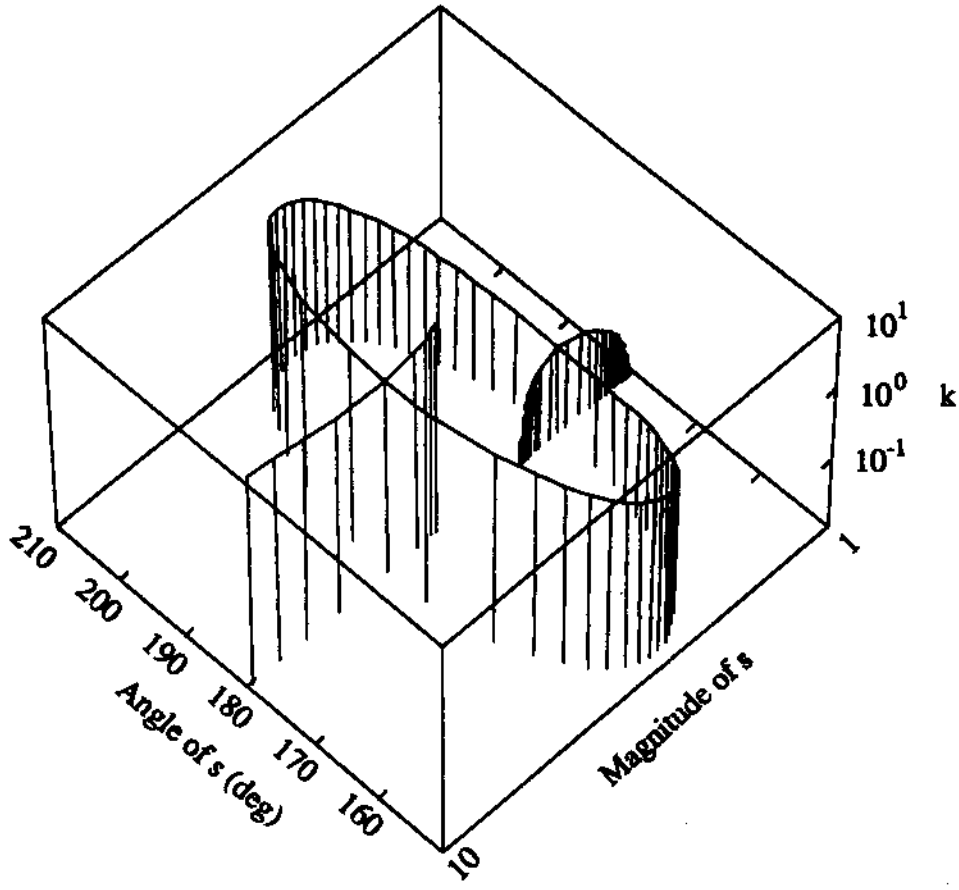

Figure 11. Three-Dimensional Gain Plot of Equation (1).

The Gain Plots (GPs)

Just as two-dimensional Bode plots simplify the three-dimensional Bode plot, two-dimensional GPs may be employed to simplify the three-dimensional Gain Plot. Figures 12a,b are such a representation for the closed-loop system embedding the system of equation (1). The Magnitude Gain Plot (MGP) is seen by viewing Figure 11 from a direction orthogonal to the k-magnitude plane and the Angle Gain Plot (AGP) is seen by observing Figure 11 from a direction orthogonal to the k-angle plane. Although the same information is presented in Figures 11 and 12, the GPs are significantly simpler to understand.

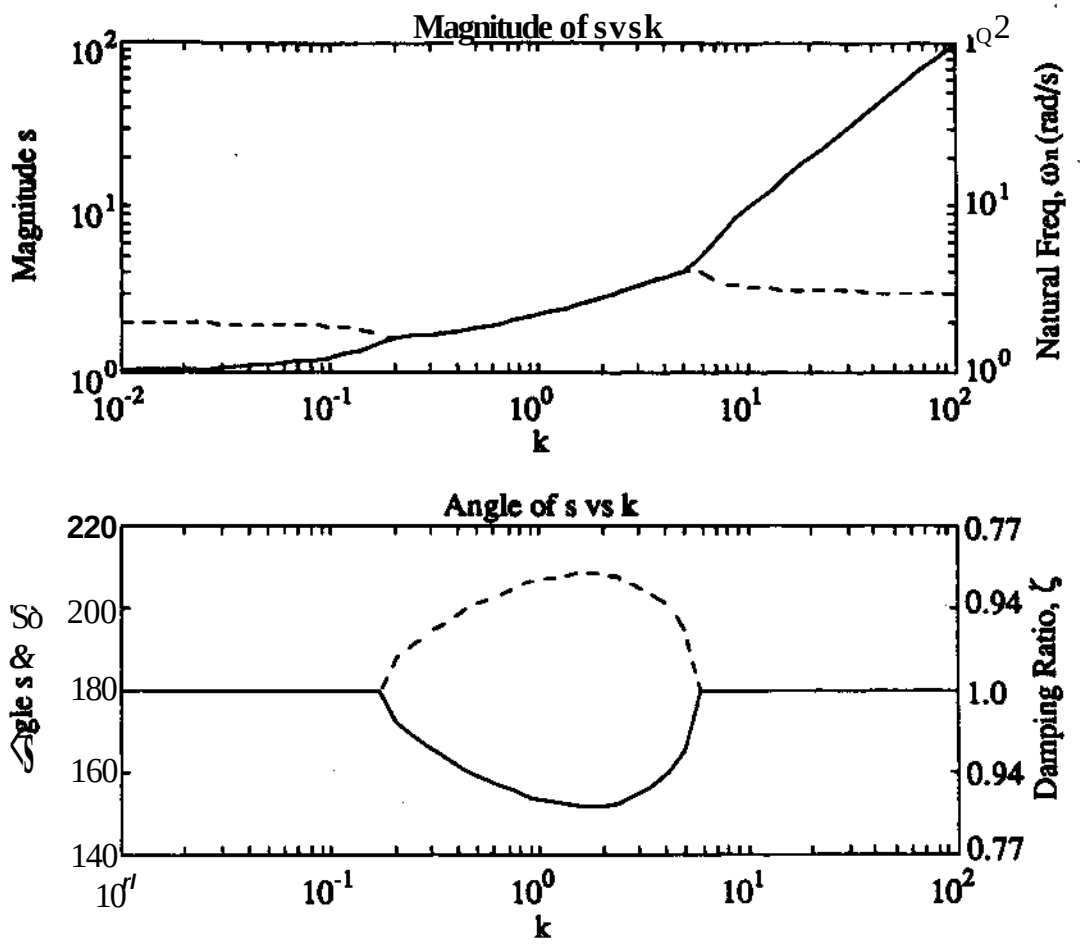

Figure 12a, b. The Magnitude and Angle Gain Plots of Equation (1).

The AGP reflects the basic construction rule of the root locus, *i.e.*, the angle criterion of equation (9). As a result, the AGP is symmetric along the 180* (=-180#) line. Furthermore, the angle criterion dictates that the eigenvalues must lie on the real axis or be complex conjugates. Thus, a pair of complex conjugate eigenvalues is shown as a single curve in the **MGP** with corresponding angles symmetrically configured about the 180* line shown in the AGP. As k varies, the complex conjugate eigenvalues may become distinct real eigenvalues, causing their angles to become equal (at a multiple of 180#) and permitting their magnitudes to differ.

The MGP shows the presence of two open-loop poles with magnitudes 1 and 2 as k _» o. It also shows a single finite transmission zero with magnitude 3 and an infinite transmission zero as k -» «>. The AGP indicates that the two open-loop poles and finite transmission zero are located in the left-half plane since they have angles of 180#.

Furthermore, the AGP shows that there is an asymptote of 180* (corresponding to the infinite transmission zero) as k -»<*».

The GPs highlight the break points corresponding to points where branches leave or enter the real axis of the root locus. For example, these break points occur at k * 0-17 and at k » 5.83. Between these break points the AGP indicates that the loci of the two branch points are not on the real axis and the corresponding single curve of the MGP confirms that the trajectories are those of a complex conjugate pair.

Properties of Gain Plots

The AGP and the MGP highlight several important stability and performance features of the system, some of which are summarized in Figures 13a,b. Stability may be determined from the AGP by noting if the angle of an eigenvalue meets the following criterion

$$180^{\#}(2m + 1) - 90^{\#} < M < 180^{\#}(2m + 1) + 90^{*} \quad , \quad m = 0, \pm 1, \pm 2, \ldots \qquad (14)$$

corresponding to a location in the second and third quadrants of the complex plane. For the case m=0, equation (14) simplifies to

$$90^{\#} < 9 < 270^{\#} \qquad (15)$$

This range is shown in the shaded region in Figure 13b.

Performance measures are presented directly by the GPs. In particular, the natural frequency, Cln (rad/s), is the magnitude shown in the MGP, and the damping ratio, £, is

$$C\text{-}|\cos\text{-}i(e)| \qquad (16)$$

where 6 is the angle from the AGP. As shown in Figure 13, supplementary axes can be added to the GPs displaying On and £. If the eigenvalues are on the real axis, the MGP presents the system time constants.

Although the conventional root locus plot provides such performance information, there are several advantages of the GPs. First, the influence of independent variable gain on ordinate (dependent) variables is exposed explicitly. Second, the performance measures of o>n and £ are represented directly. Thus, given a design specification for o>n and £, the requisite value of k may be determined by inspection making the GPs a useful graphical pole-placement tool. A novel feature of the GPs is this link of performance and gain.

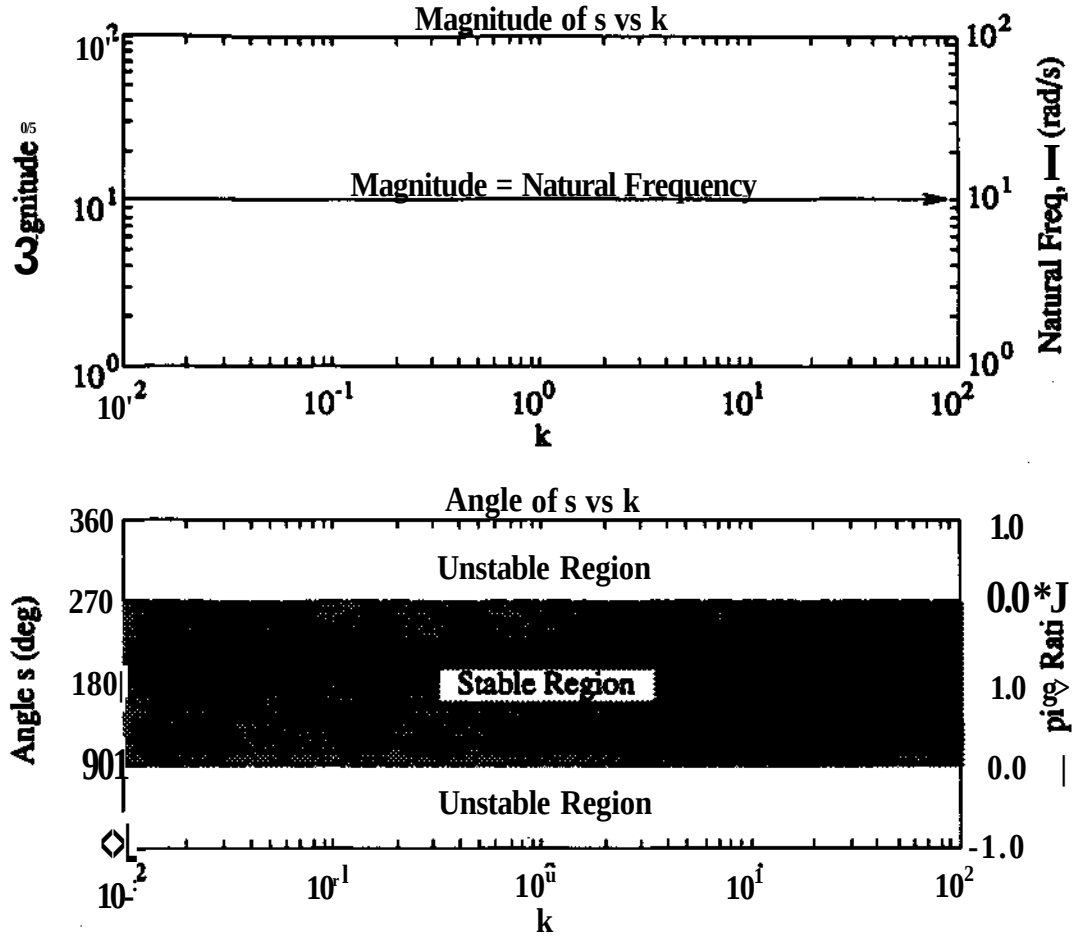

Figure 13a,b. Parameters in the Gain Plots.

The GPs are also well suited for determining eigenvalue sensitivity to changes in gain. The slopes of the GPs directly give the change in magnitude and angle of each eigenvalue per change in gain. This information is useful in the design of robust control systems that are less sensitive to gain variations. An in-depth treatment of asymptotic behavior of SISO high gain eigenvalues (and its relation to sensitivity) is covered in (Kurfess and Nagurka, 1991a).

The classical concepts of gain and phase margins have analogs using the GPs, The gain margin is the amount of gain that can be increased before the closed-loop system becomes unstable. This can be determined from the AGP by identifying the gain interval for which all eigenvalues have angles within the stable region. In principle, a system with a larger gain margin should be relatively more stable than one with a smaller gain margin. The phase margin is the largest angular interval corresponding to unity magnitude gain for which the closed-loop system is closed-loop stable. It can be determined from the AGP

by identifying **the** minimum distance from any of the poles to the unstable region at k = 1. These concepts of relative stability are the subject of a separate report (Nagurka and Kurfess, 1991b).

In addition to the advantages above, the GPs provide a unified approach for SISO and MEMO systems where compensation dynamics are governed by a single scalar gain amplifying all plant inputs. The advantage of the GPs to uniquely identify locus branches as a function of gain is of paramount importance in MIMO systems analysis, where this information is typically hidden in presenting multivariable root loci. MIMO GPs are discussed in detail in a companion report (Nagurka and Kurfess, 1991a).

Illustrative Example

This section presents a more complicated SISO example given by the open-loop transfer function

$$g(s) = \frac{(s+1)}{s(s-1)(s^2+4s+16)} \tag{17}$$

(Equation (17) is studied in example A-5-3, Ogata, 1990.) Figure 14 is the root locus plot for this system embedded in the negative feedback system of Figure 1. The root locus begins at the open-loop poles located at s={0, +1, -2 ± V3"}. The open-loop complex conjugate pole pair migrates to the real axis with increasing gain. One of these poles then proceeds to the finite transmission zero at s=-l; the other pole moves to an infinite transmission zero along an asymptote of 180*. The two real open-loop poles migrate to s»0.46, and then break out from the real axis. As a complex conjugate pole pair, they move to the left of the imaginary axis. Subsequently, they migrate back to the right of the imaginary axis and continue toward infinite transmission zeros along asymptotes of ±60*. For a small range of k, the root locus is located completely within the left half of the complex plane, corresponding to a stable closed-loop system. This range may be found from the magnitude criterion to be

$$23.3 < k < 35.7 \tag{18}$$

These gain values are not evident from Figure 14.

Figures 15a,b are the GPs for the system given by equation (17). Information about the open-loop eigenvalues at k = 0 shows *(i)* there is an unstable set of open-loop poles at an angle of 0* having magnitudes of 0 and 1, and *(ii)* there is a complex conjugate open-loop pole pair having magnitude 4 at angles of 120* and 240*. By inspection, these

complex conjugate poles have a natural frequency of 4 rad/s and a damping ratio of 0.5, although this information is "secondary" since the open-loop system is unstable. In Figure 15a,b additional vertical axes reporting natural frequency and damping ratio are shown. Negative damping ratios correspond to an unstable system.

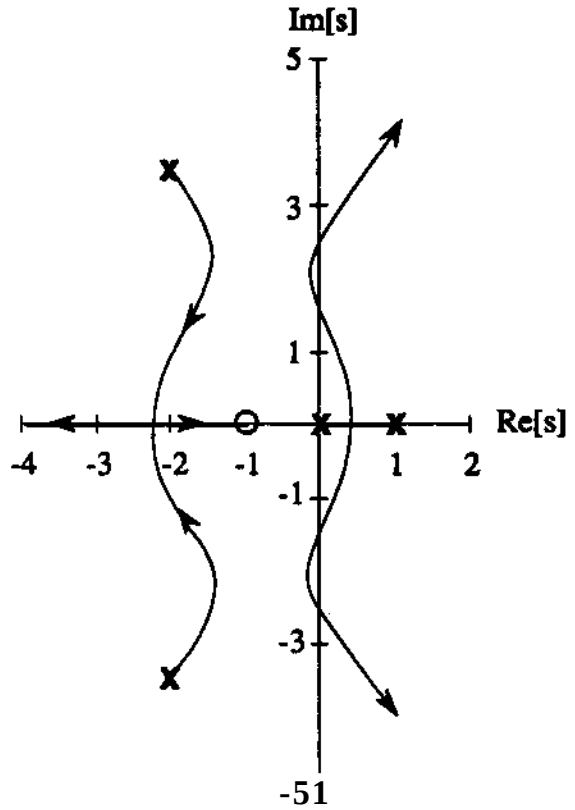

Figure 14. Root Locus Plot of Equation (17).

For positive values of gain, the system operates under closed-loop negative feedback and reveals interesting eigenvalue trajectories. For example, the solid and solid dashed lines in the MGP and AGP track the locus of the poles that start as a complex conjugate pair. The dotted and dotted dashed lines in these plots represent the locus of the pole pair that originates on the real axis. Notice that when a given pole pair is complex, the two poles have the same magnitude but are distinguished in angle. Conversely, when poles lie on the real axis, they have a principal angle of either 180* or 0* corresponding to negative or positive real values, respectively. Furthermore, the GPs show that the system is stable only for a specific range of k, matching that given in equation (18). Figure 16 is an enlargement of a section of the AGP, highlighting one of the complex conjugate poles near the stable region of the closed-loop system, from which the gains may be read

directly. **The -90* boundary** is **marked** in **the** figure in accordance with the criterion presented in **equation (14).**

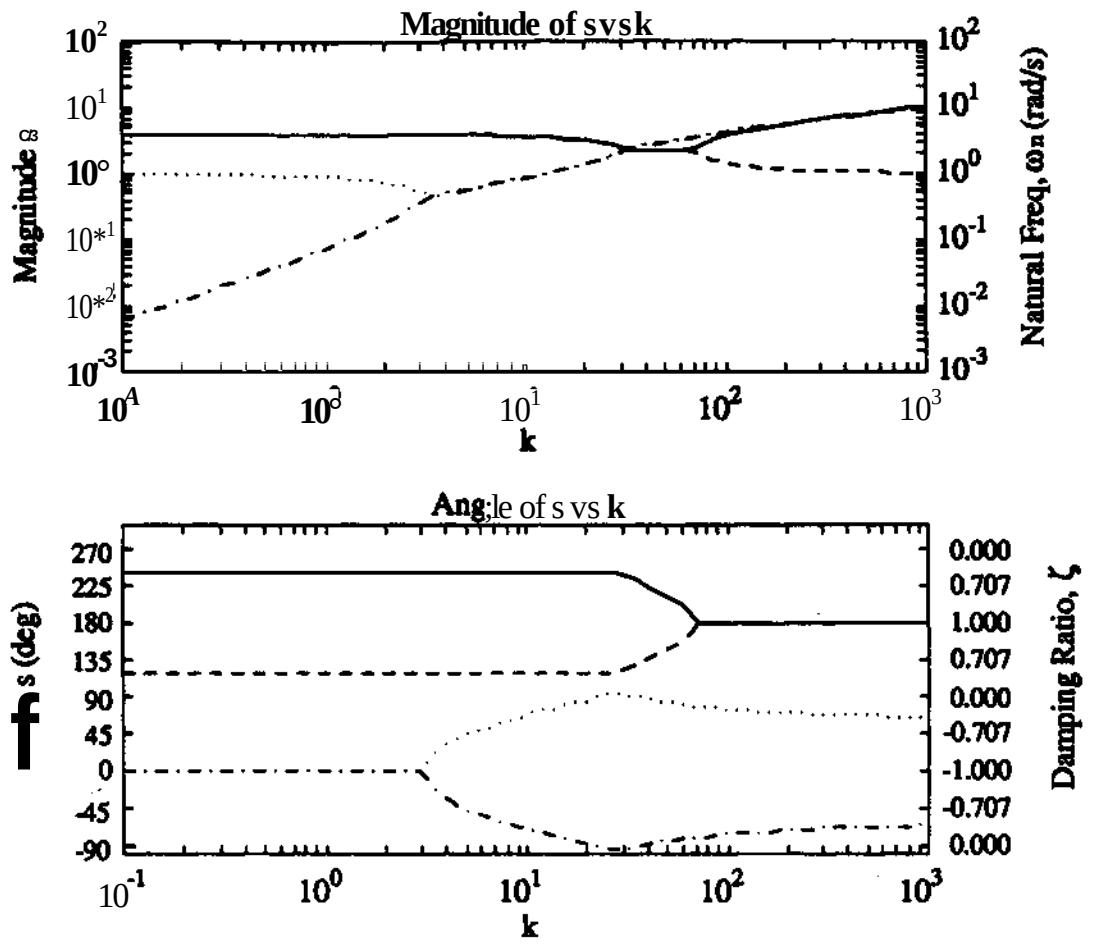

Figure 15. Magnitude and Angle Gain Plots of Equation (17).

The high gain asymptotes of the root locus are found by examining the AGP for large values of k. The finite zero at s=-l is identified by the single pole asymptotically approaching unity magnitude at an angle of 180*. The remaining three eigenvalues asymptotically approach infinite zeros at angles ±60° and 180*. For gains higher than those reported in Figure 15a,b, these asymptotes are increasingly prominent

Further inspection of the GPs provides information about the closed-loop system sensitivity to changes in gain. In the example, the system is highly sensitive to gain variations when k is small as evidenced by the rapid change in both the angle and magnitude of the system eigenvalues. This behavior is noticeable at k»3.1, where the angle of the unstable pole pair rises abruptly. Clearly, as k-** *(i)* the angles in the AGP

asymptotically approach the Butterworth configuration, and *(ii)* the magnitudes of the eigenvalues are related to the gain via a power law relationship depicted as a straight line on the MGP (Kurfess and Nagurka, 1991a).

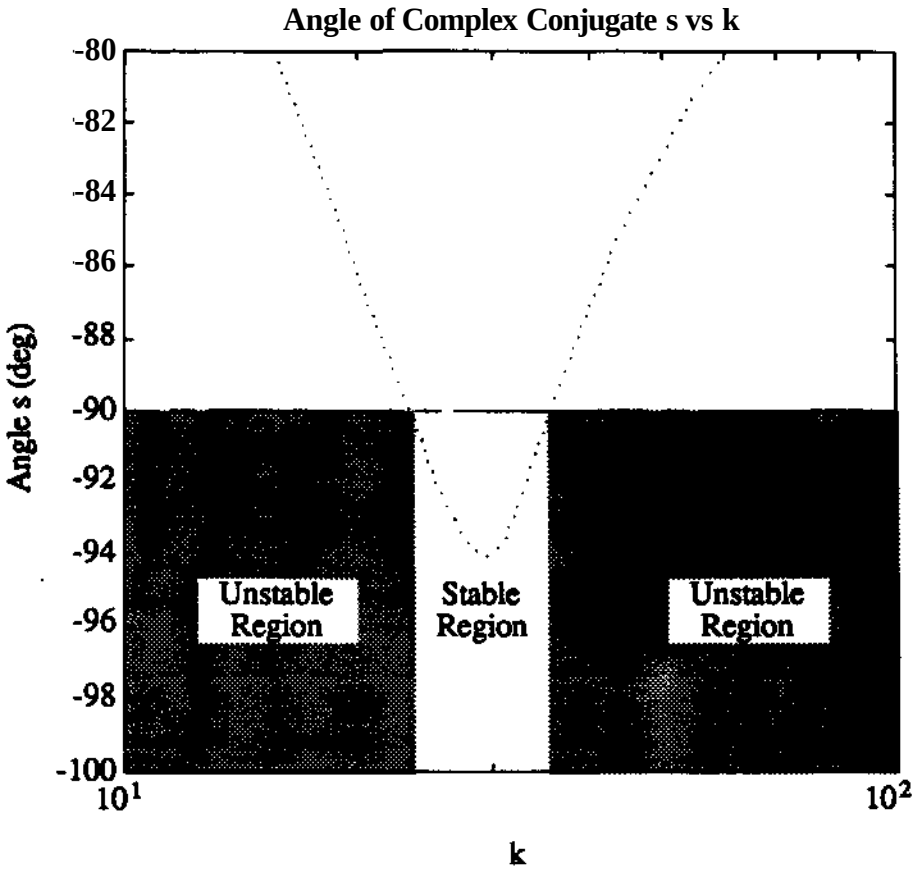

Figure 16. Expanded Angle Gain Plot of Equation (17).

Conclusions

The Gain Plots proposed in this report are a set of illuminating plots that expand and enhance the control engineers' design tool set. By presenting the magnitude and angle in separate graphs, the GPs simplify and supplement the information contained in the Evans root locus, in analogy to the role the Bode plots play with respect to the Nyquist diagram. As such, the GPs add a third "dimension" (a gain domain) to the Evans root locus plot, whereas the Bode plots add a third "dimension" (a frequency domain) to the Nyquist diagram. In the GPs, the common axis linking magnitude and argument is gain; in the Bode plots, the common axis bridging magnitude and argument is frequency.

Figure 17 highlights the correspondence of four classical controls graphical tools. As shown, **the** GPs fill what may be viewed as a "missing" quadrant of the classical controls tool **set** The first row portrays the Nyquist diagram and the Evans root locus spanning a two-dimensional complex plane. The second row shows the Bode plots and GPs spanning a three-dimensional (real) space. The columns show the variable that is used to increase the dimension, *i.e.*, frequency for Bode plots, gain for GPs. The columns correspond to the earlier progressicxi figures (Figures 3 and 8) where the three-dimensional representations have been removed. Strong connections exist between the four tools identified in Figure 17, with all tools being valuable for stability and performance evaluation.

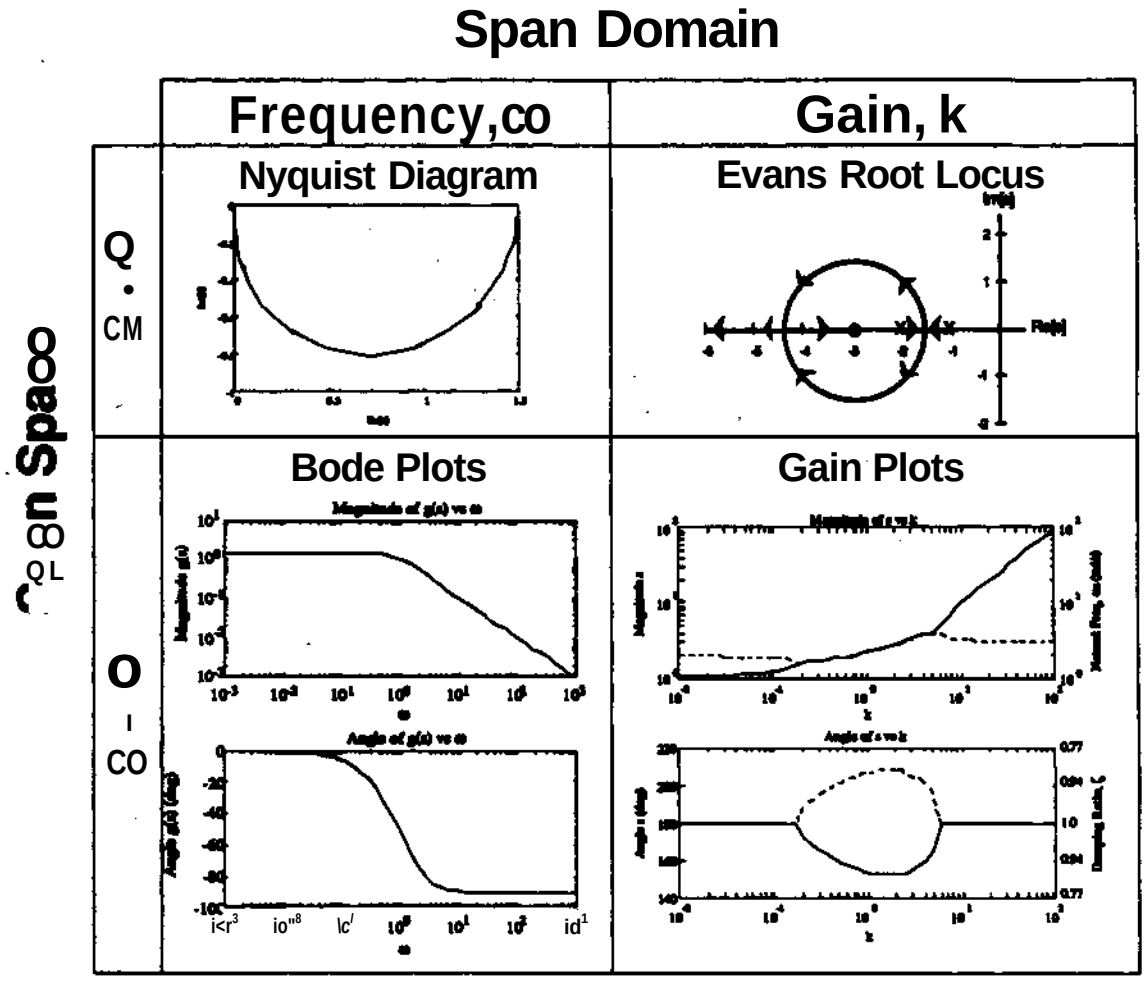

Figure 17. Quadrant Representation of Graphical Control Tools.

The proposed GPs enhance the root locus by explicitly portraying the relationship between the gain and the location of each eigenvalue whose trajectories are mapped by the

root locus. This information is not readily available from the root locus plot. The enhancement enables the control designer to identify, by observation, an eigenvalue location with a specific gain, and hence directly view the influence of the gain on stability as well as on system performance. Furthermore, the GPs provide a direct measure of eigenvalue gain sensitivity. The change in eigenvalue magnitude and angle per change in gain is indicated by the slope of the GPs. This measure of sensitivity highlights the "cost" of selecting eigenvalue locations corresponding to specific gain values, and provides the designer with a novel graphical means to assess control system robustness.

Many similarities and differences exist between the root locus and the GPs. For example, both the root locus plot and the GPs can be drawn for systems with transportation lags or dead time. Unlike the root locus plot, the GPs explicitly highlight open-loop poles near or at transmission zeros. These poles are depicted as horizontal lines indicating constant magnitude and angle for all gains. In the root locus plot pole-zero cancellations are normally camouflaged.

Current work is targeted at developing analogous "root locus" rules for sketching the GPs. Although several of these rules have been identified (including the rule for high gain magnitude asymptotes), their utility may be limited given the ability for real-time computer implementation.

Further work is necessary to develop intuitive geometric relationships between the Bode plots that present open-loop information and the GPs that present closed-loop information (for k * 0). The Nichols chart may provide the appropriate connection. It presents the relationship between the frequency response of the open-loop system and that of the closed-loop system. In so doing, it displays four dimensions of information *(i.e.*, open and closed loop gain and magnitude) in a two-dimensional format where co is the implicit variable. The Nichols chart is a challenging chart to generate and comprehend; however, it does provide a bridge between open-loop and closed-loop systems in the frequency domain. If the connection between Bode plots and GPs is made, then some of the more powerful frequency domain tools may find new applications in control theory.

In closing, controls engineers have historically embraced powerful graphical design methods with striking success. These methods supply significant insight, permitting rapid system analysis and synthesis. This report proposes a new graphical design tool, the Gain Plots, and presents a global perspective of these plots with respect to important classical control tools. The GPs provide a broad spectrum of information about the closed-loop

control system, including stability, performance, and robustness attributes, and may be viewed as a missing classical controls tool

References

Bode, H. W., 1940, "Relations Between Attenuation and Phase in Feedback Amplifier Design," Bell System Technical Journal, Vol. 19, pp 421-454.

Cannon, R. H. Jr., 1967, Dynamics of Physical Systems, McGraw-Hill, New York.

Evans, W. R., 1948, "Graphical Analysis of Control Systems/* Transactions of the American Institute of Electrical Engineers, Vol. 67, pp 547-551.

Evans, W. R., 1950, "Control System Synthesis by Root Locus Method/' Transactions of the American Institute of Electrical Engineers, Vol. 69, pp 1-4.

Kurfess, T.R. and Nagurka, M.L., 1991a, "A General Theory for High Gain Asymptotic Behavior of Eigenvalues Approaching Finite and Infinite Transmission Zeros," ASME Journal fif Dynamic Systems, Measurement and Control, *submitted.*

Kurfess, T.R. and Nagurka, M.L., 1991b, "On the Relationship Between Eigenvalue Sensitivity and High Gain Root Loci," Mechanical Engineering Technical Report

Nagurka, M.L. and Kurfess, T.R., 1991a, "Gain Plots: A New Perspective on the MIMO Root Locus," ASME Journal of Dynamic Systems, Measurement and Control, *submitted.*

Nagurka, M.L. and Kurfess, T.R., 1991b, "The Margin of the Gain Falls Mainly on the s-Plane," Mechanical Engineering Technical Report

Nyquist, H., 1932, "Regeneration Theory," Bell System Technical Journal, Vol. 11, pp 126-147.

Ogata, K., Modem Control Engineering, 1990, Prentice Hall, Englewood Cliffs, NJ.